CILAMCE 2017
Florianópolis - Santa Catarina - Brazil

GLOBAL ANALYSIS OF THE PENETRATION OF A TORPEDO ANCHOR MODELED BY PANEL MESH

Carolina Maria Nunes Bezerra

Fabrício Nogueira Corrêa

Jhonathan Jhefferson de Sousa Ribeiro

Adolfo Emmanuel Correa Lopez

Breno Pinheiro Jacob

carolmnb@coc.ufrj.br

fabricio@lamcso.coppe.ufrj.br

jj@lamcso.coppe.ufrj.br

adolfo.correa@lamcso.coppe.ufrj.br

breno@lamcso.coppe.ufrj.br

COPPE/UFRJ – Alberto Luiz Coimbra Institute for Graduate Studies and Engineering Research, PEC – Civil Engineering Program, University Campus – Fundão Island, Avenue Pedro Calmon, S/N, CEP 21941-596, Rio de Janeiro - RJ - Brazil.

Abstract. *In deep-water offshore oil exploration, the mooring foundations are usually submitted to high loads in a soil that is, usually, extremely soft. To circumvent this problem, torpedo anchor is frequently used to fix the mooring line on seabed. In this context, this paper presents a new numerical approach to represent the soil reaction of torpedo anchor, in a global analysis tool to model its installation procedure, via a numerical integral of soil pressures on its penetrated surface. Therefore, this method is associated to the weak coupling formulation in time domain, in which the torpedo is represented by a rigid body with six degrees of freedom and the mooring and launching lines are represented by finite elements. The method was developed on in-house program SITUA-Prosim and compared to the classic True model. In this numerical procedure, a typical impact velocity and physical data were used to represent a real launching procedure evaluated in Campos Basin-Brazil. The geometric factors (presence of wings) and the variation of the soil drag coefficient were evaluated as parameters of influence in the embedment depth of the anchor.*

Keywords: *Torpedo anchor, True model, Panel mesh, Shear resistance, Drag coefficient.*

INTRODUCTION

The torpedo anchor system was developed by Petrobras in order to be able to operate in offshore oil and gas production systems at depths of 2000 m (Lavieri, 2011). The torpedo anchor is a foundation system that was created to be installed by free fall in soils composed of soft clay, as well as oil fields that have been identified in deeper water such as in the Campos Basin-Brazil (Kunitaki, 2006). The torpedo anchors have demonstrated to be efficient in anchoring offshore systems and are widely used, especially in deep waters.

The torpedo anchor consists of a tubular steel section, four wings and a conical base, filled with high specific mass material. These characteristics were designed to make the anchor to achieve the kinetic energy required to penetrate significantly the soil when launched from a previously calculated depth. The launching depth of the torpedo is closely related to the geotechnical conditions of the site where the installation is required. Therefore, it is necessary to evaluate with more precision the main parameters that influence the penetration of the anchor in the soil, which are: mass, impact velocity, geometry, shear strength and damping.

In this paper, the True model (True, 1976) is used to represent the contact between the torpedo anchor and the soil during the embedment, by means of pressures integral on the surface of the torpedo modeled by panel mesh. The following factors was analyzed to evaluate the anchor penetration: the presence of wings and the soil drag coefficient. Numerical analysis considers the same geotechnical parameters and physical properties used in a project of the real T-98 torpedo installation anchor.

1 THE PENETRATION MODEL

Studies on the behavior of penetration of projectiles were initially studied for military applications. The development of a dynamic penetration model by the US navy was required to represent the penetration of propellant-embedded plate anchors into seafloor soils (Beard, 1980). This kind of anchor is directly positioned on the mud line and an explosion, caused by the propeller system, pushes the anchor fluke down. In order to fulfill this objective, True (1976) took into account recommendations given by authors of empirical models, such as Young (1969), and modified traditional bearing capacity formulations for deep foundations in cohesive soils to consider variations in penetration resistance with velocity and penetrator shape (Kunitaki, et al., 2008). The analytical model developed by True (1976) to simulate the dynamic penetration of plate anchors is based on Newton’s second law, and the governing equation can be written as follows (Eq. 1):

$$M'.v.\frac{dv}{dz} = F_E + W_S - F_D - F_T - F_S \quad (1)$$

where M' is the effective mass of the penetrator, given by Eq. 2.

$$M' = M + 2\rho V \quad (2)$$

According to the Eq. 1, v, W_S and z are the velocity, submerged anchor weight and the seafloor depth, respectively. The penetrator velocity v can be expressed as $v = dz/dt$, where (z stands for the soil depth), and therefore, its acceleration dv/dt can be expressed as $(dv/dz)(dz/dt)$. F_E is the external driving force applied by the propeller system, F_D is the drag resistance, F_T is the axial tip reaction and F_S is the side friction force.

In the Eq. 2, M, V and ρ are the structural mass, the volume of the penetrator and the mass density of the soil, respectively. The term $2\rho V$ is similar to the "added mass" term of the Morison equation (Morison, et al., 1950), which has been traditionally employed to calculate hydrodynamic drag and inertia loads on cylinders immersed in fluid. When the term $2\rho V$ is multiplied by the acceleration at the left side of the Eq. 1, it is introduced an additional inertia force that corresponds to the contribution of the soil in which the penetrator is immersed.

However, in the studies of free-falling cylindrical penetrometer, dropped from a given height above the mudline for the prediction of penetration, the Equation (1), with some modifications, can be also applied to describe the movement of this penetrometer (Beard, 1981). Firstly, there is no external driving force due to free falling, thus, the term F_E is omitted. Also, the added mass (Eq. 2) is considered negligible for slender penetrometers moving along their long axis, thus, the effective mass M' is equal to the structural mass M. Therefore, replacing the velocity v by dz/dt and considering that the acceleration a is equal to $(dv/dz)(dz/dt)$, the Equation (1) can be rewrite:

$$M.a = W_S - F_D - F_T - F_S. \quad (3)$$

The submerged weight W_S is represented by Eq. 4:

$$W_S = W - V.\gamma \quad (4)$$

where M, W and V are, respectively, structural mass, weight in the air and the volume of the anchor; and γ are the specific weight of the submerged soil.

1.1 Soil parameters for dynamic penetration

1.1.1 Soil strain rate

The strain rate factor $S_{\dot{e}}$ of the soil is an empirical expression derived by True (1976) from the tests penetration data, defined as a function of the velocity v and the diameter (or thickness) of the penetrator d, the undrained soil shear strength S_u, and other empirical parameters according to Equation (5).

$$S_{\dot{e}} = \frac{S_e}{1+\frac{1}{\sqrt{\frac{C_{\dot{e}}.v}{S_u.d}+C_0}}} \geq 1 \quad (5)$$

The undrained shear strength S_u of the soil is assumed to vary linearly with depth z

$$S_u(z) = S_{u_0} + S_{u_k}.z \quad (6)$$

Values for the empirical parameters Se (maximum soil strain rate at high velocity values), $C_{\dot{e}}$ (strain rate velocity factor), and C_0 (strain rate constant) were also determined based on results of model tests (True, 1974).

1.1.2 Soil resistance forces and inertial drag

The soil resistance forces in the right-hand side of the Equation (3) are the tip resistance F_T and the side resistance F_S, which are expressed as:

$$F_T = (S_u.N_c.A_T).S_{\dot{e}} \quad (7)$$

$$F_S = \left(\frac{S_u.A_S.\delta}{S_{ti}}\right).S_{\dot{e}} \quad (8)$$

where A_T and A_S are, respectively, the frontal and lateral areas of the anchor pile. The soil sensitivity value is given by S_{ti}, which represents the loss of shear strength that clays suffer when remolded, and is defined as the ratio of undisturbed and remolded strengths (Skempton, et al., 1952). N_c is the bearing capacity factor (assumed equals to 9 for homogeneous clay) and δ is a side adhesion reduction factor. Values for the side adhesion reduction factor δ were determined in based on results of model tests (True, 1974).

The drag force F_D is like the longitudinal drag component given by Morison's equation (Morison, et al., 1950), however, considering ρ as the soil density. The drag force comprises a pressure drag component due to the pressure exhibited on the tip of the object and a friction drag component due to the shear stresses acting along the cylindrical surface of the object. Generally, the effects of pressure and friction drag are combined and an overall drag coefficient C_D (Richardson, 2008) can be considered as follows:

$$F_D = \frac{1}{2}.v.|v|.A_P.C_D.\rho \quad (9)$$

1.2 Original solution procedure of True equation

To solve (3), True developed an incremental finite-difference algorithm and considered that the penetrator is a point object at *i*th time increment, thus some simplifications could be made:

$$M'.\frac{v_{i+1}-v_i}{\Delta t} = W_s - F_D - F_T - F_S \quad (10)$$

Substituting the expressions M', W_s, F_D, F_T and F_S, the following is obtained, which can be applied repeatedly to obtain the velocities of the penetrator at each time increment Δt:

$$v_{i+1} = v_i + \frac{\Delta t}{M}.\left[(W - V.\gamma_S) - \left(\frac{1}{2}.v_i.|v_i|.A_P.C_D.\rho\right) - S_{u_i}.\left(A_T.N_c + \frac{A_S}{S_{ti}}\right).\left(\frac{S_e}{1+\frac{1}{\sqrt{\frac{C_{\dot{e}}.v_i}{S_{u_i}.d}+C_0}}}\right)\right]$$

(11)

The final penetration depth can then be seen as the product of the time increment Δt by the number of the increment for which the penetrator velocity drops to zero. It should be recalled that, as in any numerical solution procedure, the accuracy of the results also depends on the careful selection of the time increment. This will depend on the particular example that is analyzed, and may also involve the use of different increment values to assess the convergence to an accurate solution.

2 PANEL MESH METHOD

The panel mesh method consists of a numerical procedure for the calculation of the integrals of pressures due to the action of the soil on the anchor surface during the embedment. In this work, these pressures are generated by the equation of True calculated locally for each mesh element. This method was developed on in-house program SITUA-Prosim (Jacob, et al., 2006), implemented in FORTRAN programming language.

In this procedure, the torpedo is represented by a mesh of triangular elements. When the anchor touches the soil surface, starting its penetration, the program identifies the elements below the soil, represented by a local plane equation. Then, in each vertex of the triangular elements the pressures are calculated, due to action of the soil buoyancy, normal and tangential stress due to the drag and soil resistances − derived from the expression at the right side of the True equation (Eq. 3).

Although the True Model uses global coefficients to represent the soil, those coefficients were assumed, as approximation, in the normal and tangential direction of each element of the panel mesh with the objective to transform the main forces of the True model in pressure/stress effects on element.

The soil resistance and drag effects have been calculated considering the normal (v_N) and tangential (v_t) velocity on each vertex of the triangular element due the rotation and translation displacements of the torpedo represented by a rigid body. The True equations of the pressures due the resistance and drag forces of the soil can be modified as follows, respectively:

$$p_N = (S_u . N_c) . S_{\dot{e}}(v_N) \tag{10}$$

$$p_t = \left(\frac{S_u . \delta}{S_{ti}}\right) . S_{\dot{e}}(v_t) \tag{11}$$

$$p_{DN} = \frac{1}{2} . v_N . |v_N| . C_{DN} . \rho \tag{12}$$

$$p_{Dt} = \frac{1}{2} . v_t . |v_t| . C_{Dt} . \rho \tag{13}$$

The Figure 1-a illustrates schematically a part of the torpedo below the soil, modeled by panel mesh and the Figure 1-b illustrates a triangular element with pressures evaluated on its vertex, showing the pressure center as a red point.

The integral of these pressures is calculated for each triangular element (Figure 1(b)) providing the resultant forces in the pressure center of each element. It is important to note that the pressures could be calculated, by approximation, on the barycenter of the triangular element. However, the integration procedure illustrated in Figure 1(b), considering the application of the force in the in the center of the volume of pressures, is more accurate. In this way, the accuracy of the method is increased and allows the use of a reduced number of elements to represent the continuous surface of the torpedo.

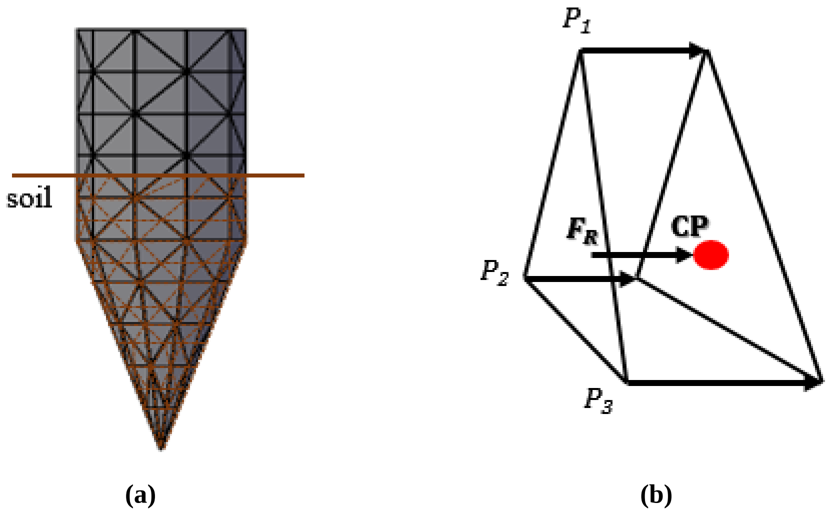

Figure 1: (a) Final section of the torpedo anchor displaying the panel mesh; (b) Volume of pressures on triangular element of the mesh.

The forces acting on each element are transferred to the center of gravity (GC) of the torpedo, producing a resultant moment. Next, the resultant forces and moments of all penetrated elements are applied on the right-hand side of the dynamic equation of the rigid body represented by the six degrees of freedom of the torpedo (Kunitaki, 2006). This procedure is evaluated for each time-step of the time domain simulation.

3 COMPUTATIONAL ANALYSIS

3.1 Model Validation

The application of the penetration model validation corresponding to a pile dropped from a height of 170m above the seabed. The torpedo and the soil data is presented in Table 1 andTable 2. It should be emphasized that the soil parameters are related to a specific soil and may not necessarily be representative of general applications.

Table 1. Torpedo Anchor data

Torpedo data	Nomenclature	Value
Weight in the air	W	961,4kN
Submerged weight in the soil	W_S	777,9kN
Length	L	17,0m
Diameter	d	1,7m

Table 2. Soil parameters

Soil parameters	Nomenclature	Value
Specific weight of the submerged soil	γ_S	6,0kN/m³
Undrained shear strength at the soil surface	S_{u0}	5,0kPa
Rate of increase with depth	S_{uk}	2,0kPa/m
Sensitivity	S_{ti}	3,5
Bearing capacity factor	N_C	9,0
Side adhesion reduction factor	δ	0,9
Empirical maximum strain rate factor	S_e	5,0
Empirical strain rate velocity factor	C_e	0,02kN.s/m²
Strain rate constant	C_0	0,06

In this case study, only the torpedo anchor was modeled – no line was considered – to focus the results only on the numerical integration procedure. Therefore, in order to take into account the increase of drag effects due to the mooring line into the soil that are not explicitly represented, the model employs a value for the normal drag coefficient C_D equal to 2.7, larger than the value of 0.7 as proposed by True. The tangential (longitudinal) drag coefficient, C_{Dt}, was neglected in this study. The time domain solution is a total time of 12 seconds and the analysis is performed with a time increment of 0.001 seconds.

The validation of the numerical implementation (SITUA-Prosim) was made comparing its results evaluated by a cylindrical mesh (without tip and wings) with those evaluated by the classical True model, coded in the mathematical program *Mathcad*. The results are presented in the Figure 2, showing the vertical position of the torpedo associated with its velocity. According to the Figure 2, it is possible to conclude the numerical integral of pressures applied to the cylindrical torpedo anchor can generate very similar results calculated by the classical True model.

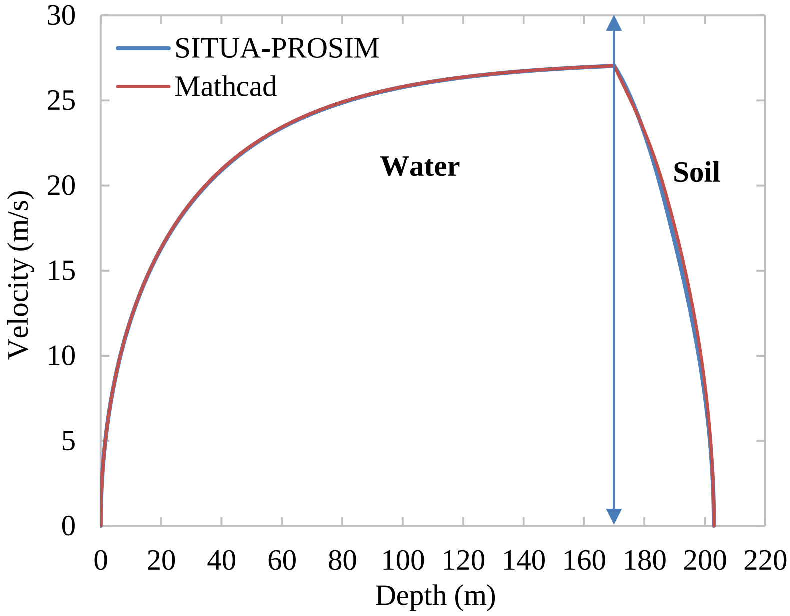

Figure 2: Model Validation – Torpedo penetration analysis (cylinder body).

3.2 Influence of geometry and normal drag force

The present study considers the launching analysis of the torpedo anchor considering two geometrical models (Figure 3): one with tip and no wings and the other with tip and four wings, the last one, geometrically equivalent with a real torpedo anchor. The objective of this study is to analyze the influence of the geometry and the drag force action in the final embedment depth of the models. The geometric factors are the tip and four wings of the anchors.

In addition, for the dynamic anchor penetration, it is assumed three different drag coefficient C_{DN}: 0, 1.26 and 2.7. These values were chosen to quantify its influence in the final penetration depth; however, the latter drag value was considered in the studies presented by Kunitaki (2006) for the numerical analyses on the prediction final embedment depth for torpedo anchor. The total penetration presented by Kunitaki (2006) was similar with the embedment depth of the torpedo T-98 realized in a real installation project of the P-50 platform, in the soft clay of the Albacora Leste Field, in the Campos Basin (Brazil). The impact velocity detected on the soil was 27m/s and was the same assumed for all models of the present study. It was possible adjusting the drop height of each model only to guarantee the same impact velocity, once the dynamic behavior of the torpedo before the impact is not the objective of this work.

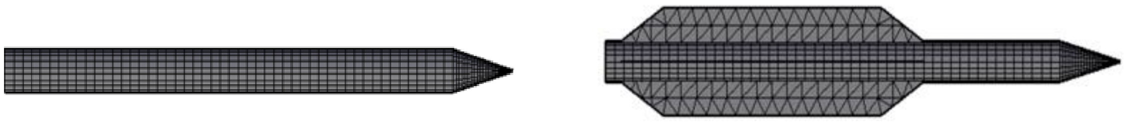

Figure 3: Model A and Model B, respectively.

The torpedo geometrical data is presented in the Table 3. Both the models have the same weight (in the air and submerged) and diameter, presented on the Table 1.

Table 3. Geometric data of the models.

	Model A	Model B
Length of the shaft	15,0m	15,0m
Length of the wings	-	10,0m
Thickness of the wings	-	0,05m
Length of the tip	2,0m	2,0m

The drop height was set up for both models achieve the same impact velocity on the seabed. According to the graph of Figure 4, it is possible to observe the influence of the variation of the drag coefficient on the total displacement of the torpedo inside the seafloor soil. The increase of the drag force contributes to increase the total shear resistance of the soil and the graph shows that the deceleration of the torpedo increases with higher values of drag coefficient. The reference used to measure the displacement of the anchors during penetration is the distance between the anchor tip and the seafloor surface.

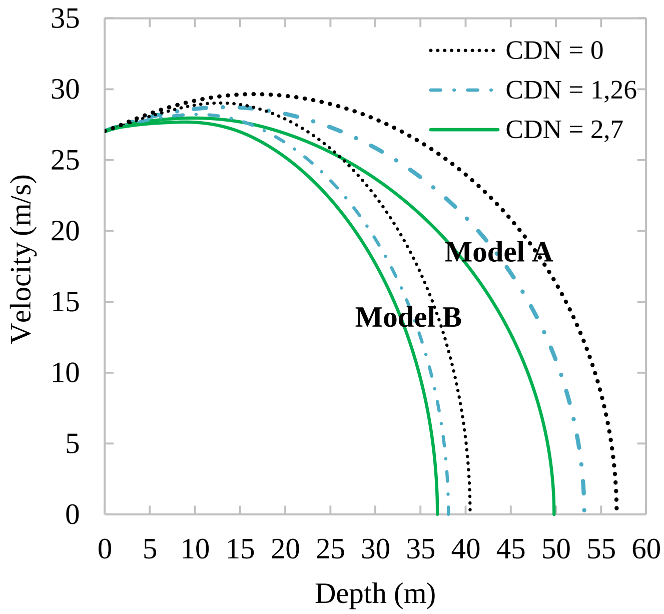

Figure 4: Displacement of the models according to each C_D value

In the initial penetration of the models A and B (Figure 4) it can be observed an overlapping of the curves between 0 and 6 meters of displacement because in this region the geometric surface of the torpedo anchor is the same for both models (between the end of the tip and the beginning of the wings – region **a** and **b** presented in Figure 6). When the wings begin to penetrate the soil (region **c** of the Figure 6), the penetration velocity begins to decrease with respect to the model B, and this reduction becomes more significant when the entire torpedo anchor is inside the seafloor. The four wings increase the area to 61.92m², increasing the soil reaction force, reducing the embedment depth. The drag force variation is presented in Figure 5.

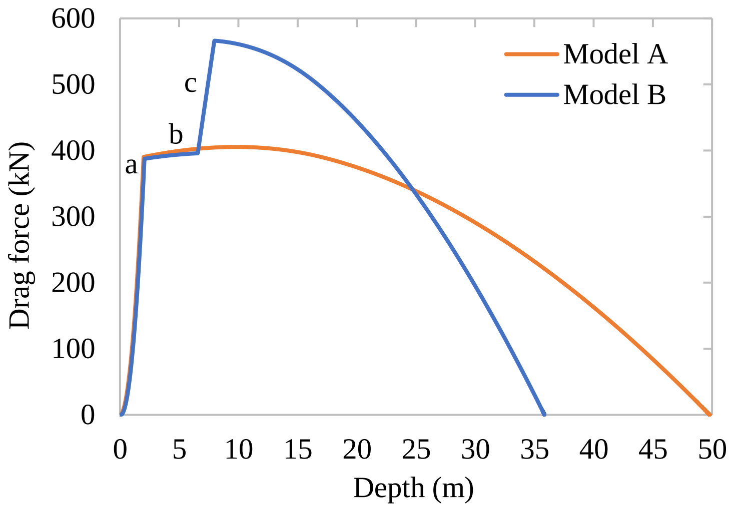

Figure 5 Drag force variation (for C_D equal to 2.7)

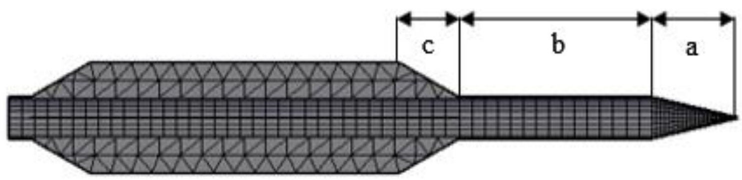

Figure 6 parts a, b and c: influence on the drag force

The total displacement variation of A and B models, considering the C_{DN} equal to 0 and 2.7, were 6.9m and 3.6m, respectively. Another interesting detail is the increase of the velocity of the anchors in the soil during the initial displacement, as shown in Figure 4. The increase in velocity during the initial of penetration is due to the fact the submerged weight is greater than the soil resistance and drag forces. This effect is reduced with the increase of drag coefficient C_D (O'Loughlin, et al., 2013).

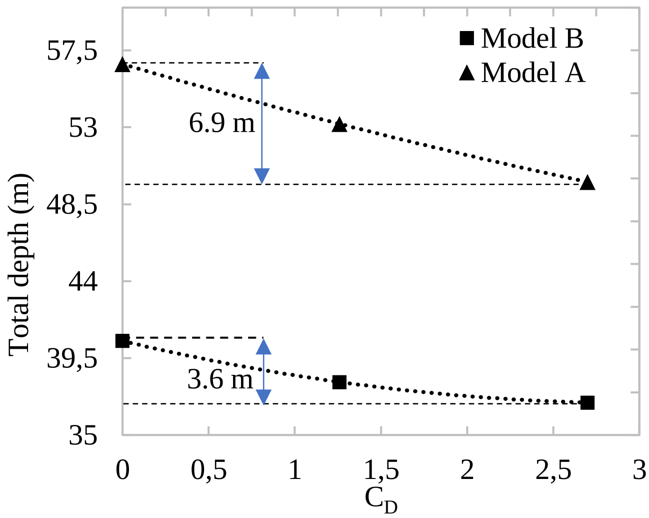

Figure 7: Total displacement of the anchor models in the soil according to C_D value

According to the graph of the Figure 8 (a), the drag force F_D has the main resistance during the instants where the torpedo anchor is penetrating the soil. After this, the drag force decreases with lower values of velocity while the soil resistance forces continue to increase, surpassing the submerged weight of the torpedo anchor until stop the movement. The interval corresponding to the increase of the anchor velocity, according to Figure 8 (b), is 0 to 9.3m, approximately. After this, the resistance forces to the movement of the anchor exceed the submerged weight. This trajectory can be seen clearly in the graph of Figure 4, e.g., for model B with C_{DN} equal to 2.7. At a depth around 17m, the torpedo anchor volume inside the soil does not change because it is entirely submerged and, consequently, the torpedo weight becomes constant (Figure 8 (a)).

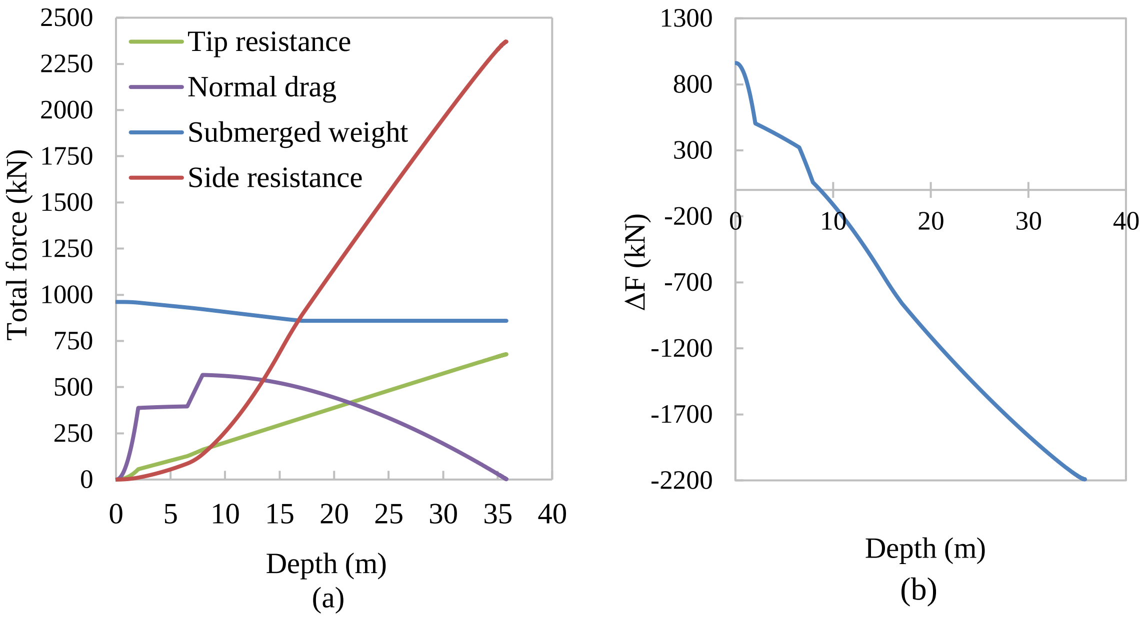

Figure 8: Model B with C_D = 2.7

4 CONCLUSION

In this work, a new numerical approach was presented to represent the soil reaction of torpedo anchor, in a global analysis tool to model its installation procedure, via a numerical integral of soil pressures on its penetrated surface. Panel mesh was used to model the torpedo anchor surface to calculate the pressures generated from the True equation. Although the True Model uses global coefficients to represent the soil forces, those coefficients were assumed, as approximation, in the normal and tangential direction of each element of the panel mesh with the objective to transform the main forces of the True model in pressure/stress on element.

The influence of the surface in the embedment depth and the application of the pressure/stress resistance on element level of the panel mesh increase the potential of this method to be used to integrate pressures evaluated from the fluid-structure interaction using any other type of formulation, such as the finite element method or method of particles to represent the soil.

The computational method presented has showing efficient and accurate results to be used in a global analysis in the design of anchor systems based on torpedo anchors.

In future works the results of this method will be compared with those observed by experimental tests, and the influence of discretization of the panel mesh on the embedment depth and on computational cost will be quantified.

ACKNOWLEDGEMENTS

The authors thank LAMCSO-UFRJ for the technical support for the development of this paper and the CAPES for the financial support.

REFERENCES

Beard R M A Penetrometer for Deep Ocean Seafloor Exploration [Artigo] // Proceedings of the 1981 IEEE/MTS Oceans Conference. - San Diego, CA : [s.n.], September de 1981. - Vol. 3. - pp. 668 - 673.

Beard R M Holding capacity of plate anchors [Conference]. - Port Hueneme, Calif, USA : Tech. Rep. R-882, Civil Engineering Laboratory, 1980.

Jacob Breno Pinheiro, Corrêa Fabrício Nogueira and Coutinho Daniel Costa e Silva PROSIM: Simulação numérica do comportamento de Sistemas Offshore para exploração de petróleo [Report]. - Rio de Janeiro, RJ. : CENPES/PETROBRAS e LAMCSO/UFRJ, 2006.

Junior Edio Soares Pereira Análise de Confiabilidade na Cravação de Estacas de Concreto Pré-Moldado [Report] / Universidade Estadual do Norte Fluminense Darcy Ribeiro, Dissertação de M.Sc.. - Niterói, RJ, Brasil : [s.n.], 2003.

Kunitaki Denise Margareth Kazue Nishimura Tratamento de Incertezas no Comportamento Dinâmico de Estacas Torpedo para Ancoragem de Sistemas Flutuantes na Explotação de Petróleo Offshore [Relatório] / Dissertação de M.Sc., Universidade Federal do Rio de Janeiro, COPPE, Programa de Engenharia Civil. - Rio de Janeiro, RJ, Brasil : [s.n.], 2006.

Lavieri R S Métodos de Navegação Inercial Aplicados a Lançamentos Submarinos [Report]. - São Paulo, SP, Brasil : Dissertação de M.Sc., Universidade de São Paulo, 2011.

Medeiros C J Torpedo anchor for deep water [Report]. - Rio de Janeiro, RJ, Brazil : Proceedings of the Deep Offshore Technology Conference, 2001.

Morison J R [et al.] The Force exerted by Surface Waves on Piles [Article]. - May 1950. - Vol. 2. - pp. 149 - 154.

O'Loughlin Conleth and Gaudin Christophe Penetration of Dinamically Installed Anchors in Clay [Article] // Géothecnique. - [s.l.] : Géothecnique, 2013.

Polo F C J Estudo das Características Estocásticas do Roll Paramétrico [Report]. - Rio de Janeiro, RJ, Brasil : PhD thesis, COPPE/UFRJ, Ocean Engineering Program, 2017.

Richardson Mark Damian Dynamically Installed Anchors for Floating Offshore Structures [Report]. - [s.l.] : University of Western Australia. PhD Thesis., 2008.

Skempton A W and Northey R D The sensitivity of clays [Article]. - [s.l.] : Geotechnique, 1952. - 1 : Vol. 3.

True D. G. Undrained Vertical Penetration into Ocean Bottom Soils [Relatório] / Ph.D. Thesis, University of California. - Berkeley, California : [s.n.], 1976.

True Daniel G Rapid Penetration into Seafloor Soils [Report]. - Houston, Texas, USA : [s.n.], 1974. - pp. 607 - 618.